



*Supplement of*

## **Spatial variability of marine-terminating ice sheet retreat in the Puget Lowland**

**Marion A. McKenzie et al.**

*Correspondence to:* Marion A. McKenzie ([marion.mckenzie@mines.edu](mailto:marion.mckenzie@mines.edu))

The copyright of individual parts of the supplement might differ from the article licence.

## Contents of this file

	S1
	Figures S1 and S2
5	Tables S1, S2, S3, S4, S5

## Introduction

The contents here within contain additional text on sample collection, preparation, and age determination of optically stimulated luminescence samples (Sect. S1). The results of the OSL data are less reliable than those of the radiocarbon dates. We lack nuclide information for adjacent layers of OSL taken on unit boundaries and faced feldspar contamination in samples. While there is some partial disagreement between radiocarbon and OSL dates, the OSL dates are still highly useful in providing approximate rates of landscape evolution based on bracketed ages of landscape emergence and submergence (Fig. 3).

Fig. S1 exemplifies the difference between lenses and laminations identified in the field. Fig. S2 showcases magnetic susceptibility data collected for each field site.

Table S1 is a compilation of site information and sample types collected. Table S2 includes the radiocarbon ages used to determine local marine reservoir effect (MRC). Table S3 is the OSL measurement sequence used for age determination.

---

**S1.** Detailed text outlining OSL sample collection, processing, and age determination.

### **S1.1 Sample collection and preparation**

Sediment samples were collected across unit boundaries with coarse-grain quartz material. To avoid pre-mature bleaching OSL, samples were collected before sunrise or after sunset, were only exposed to low energy red light, and were wrapped in opaque black plastic before being transported to East Carolina University (ECU) for preparation and processing. Sample preparation was carried out under dark-room conditions using standard coarse-grain procedures: samples were wet-sieved at 90-125  $\mu\text{m}$  with some expansion to grain sizes of 63-212  $\mu\text{m}$ . After drying the samples at 50  $^{\circ}\text{C}$ , the samples were treated with 10 % hydrochloric acid (HCl) and 29 % hydrogen peroxide ( $\text{H}_2\text{O}_2$ ). A high-density separation was conducted with lithium heteropolytungstate (LST) at a density of 2.72-2.75  $\text{g}/\text{cm}^3$  to isolate quartz grains. Coarse grains were etched for 40 minutes with 48% hydrofluoric acid (HF) to remove outer parts affected by alpha radiation, followed by a 10% HCl rinse to remove fluoride precipitates. A low-density separation to isolate quartz from feldspar was conducted with LST at a density of 2.62  $\text{g}/\text{cm}^3$ . After final sieving, the aliquots were prepared by using Reusch Silkospray to adhere material to the stainless-steel sample cups.

30 Bulk sediment was collected from outcrops for gamma spectrometry measurements and stored for at least 4 weeks prior to measurement. While the OSL samples were taken at unit boundaries, the dose rate samples were taken from the same unit as the OSL samples. Therefore, the gamma dose rates reflect the sample unit only and contain no information about adjacent, underlying, or overlying units.

### S1.2 Age determination

35 Dose measurements were conducted using a Risø TL/OSL-DA-20 reader manufactured by Risø National Laboratory with a bialkali PM tube (Thorn EMI 9635QB). The built-in  $^{90}\text{Sr}/^{90}\text{Y}$  beta source gives a dose rate of  $\sim 100$  mGy/s. Optical stimulation was carried out with an IR LED array at 870 nm with  $121$  mW/cm<sup>2</sup> (90 %) power at the sample, a blue LED array at 470 nm with  $74$  mW/cm<sup>2</sup> (90 %) power at the sample and a 7.5 mm Hoya U-340 detection filter (290-370 nm; Bøtter-Jensen & Murray, 1999). Equivalent doses were determined following the single-aliquot regenerative dose (SAR) procedure developed by Murray and Wintle (2000) and Wintle and Murray (2006). Due to feldspar contamination, a post-IR procedure was used to isolate quartz signals in the equivalent dose measurements (Wallinga et al., 2002). The preheat temperature of 180 °C for 10 s was determined for each sample using plateau and dose recovery tests. Our specific measurement protocol is outlined in Table S3.

40 Luminescence signals  $L_i$  and  $T_i$  were determined by integrating over the first 0.8 seconds of an OSL decay curve and subtracting an average of the next 4 seconds as background signal. The signal uncertainty followed from counting statistics. The sensitivity corrected signal is given by  $C_i = L_i/T_i$ . The dose response of every aliquot was determined by fitting the luminescence signals  $C_1$  to  $C_5$  with a saturating exponential. The dose  $D_0$  corresponding to the natural sensitivity-corrected luminescence signal  $C_0$ , was calculated with the fitting parameters. All uncertainties were calculated using the Gaussian law of error propagation and Poisson statistics. Most aliquots passed the reliability test – requiring recycling ratios between 0.9 and 1.1, dose recovery <10 % deviation from given dose, low recuperation. The samples had very low signals and many of the aliquots did not pass the reliability tests. The equivalent dose  $D_e$  was determined for each site using the central age model (Galbraith et al., 1999). The full uncertainty also includes 3.1 % for the built-in beta source error. Results for measurements of the equivalent dose are listed in Table S4.

50 In the sediment, grains are exposed to natural gamma and beta radiation from uranium,  $^{232}\text{Th}$ , and potassium. The concentrations of these radionuclides were measured with high resolution gamma spectrometry. Uranium concentrations determined from  $^{234}\text{Th}$  were all significantly higher than concentrations determined from  $^{214}\text{Pb}$  and  $^{214}\text{Bi}$ . We assumed that  $^{234}\text{U}$  was leached out of the sample due to in situ water presence. Dose rates were calculated by using the actual measured concentrations for the nuclides in the uranium decay chain. Uncertainties were calculated based on the maximum and minimum values obtained from the measured concentrations of  $^{234}\text{Th}$  and  $^{214}\text{Bi}/^{214}\text{Pb}$ . IR depletion during dose measurements alerted us to the possible presence of a feldspar contamination in the quartz samples. This was confirmed by subsequent visual inspection of the grains under a microscope. The fraction of K-feldspar in the quartz samples was determined visually. Potassium feldspars are assumed to have a typical concentration of 12.5% K. This number was multiplied by the fraction of K in the sample, listed in Table S5. For example, a sample for which the K-fraction was found to be 0.5 the internal potassium was assumed to be  $12.5\% * 0.5 = 6.25\%$ .

55

60 Water contents were measured as the ratio of weight water/ weight dry sample. Water contents were very low and have an uncertainty of 5 % (Table S5). Beta and gamma dose rates were calculated using the conversion factors published by Guérin et al. (2011). The cosmic dose rate was calculated as described by Prescott and Stephan (1982), Barbouti and Rastin (1983), and Prescott and Hutton (1994) and incorporates site latitude, longitude, site altitude, and sample depth below surface. The effective thickness was assumed to be half the burial depth with uncertainty of 5 %.

65 The sample ages, calculated in calendar years, were calculated by dividing the dose by the dose-rate (Tables S3, S4, S5). Some of the samples showed fading. For those, fading rates (g-values) were determined (Table S4) and the ages were corrected as suggested by Auclair et al. (2003). For those samples, ages are listed before and after fading correction (Table 2). While  $^{14}\text{C}$  ages are reported in kilo years ago (kya) calendar year BP (1955), all OSL ages are reported in kya based on the date of collection (2020). OSL ages in kya can be directly compared to kya cal. BP by subtracting 72 years from the OSL age.



70 **Figure S1.** A clay lamination seen in Unit 3 of Fort Casey Site 1 (left) and a silt lens seen in Unit 1 of Fort Casey Site 1 (right). This distinction is maintained throughout all site stratigraphic descriptions.

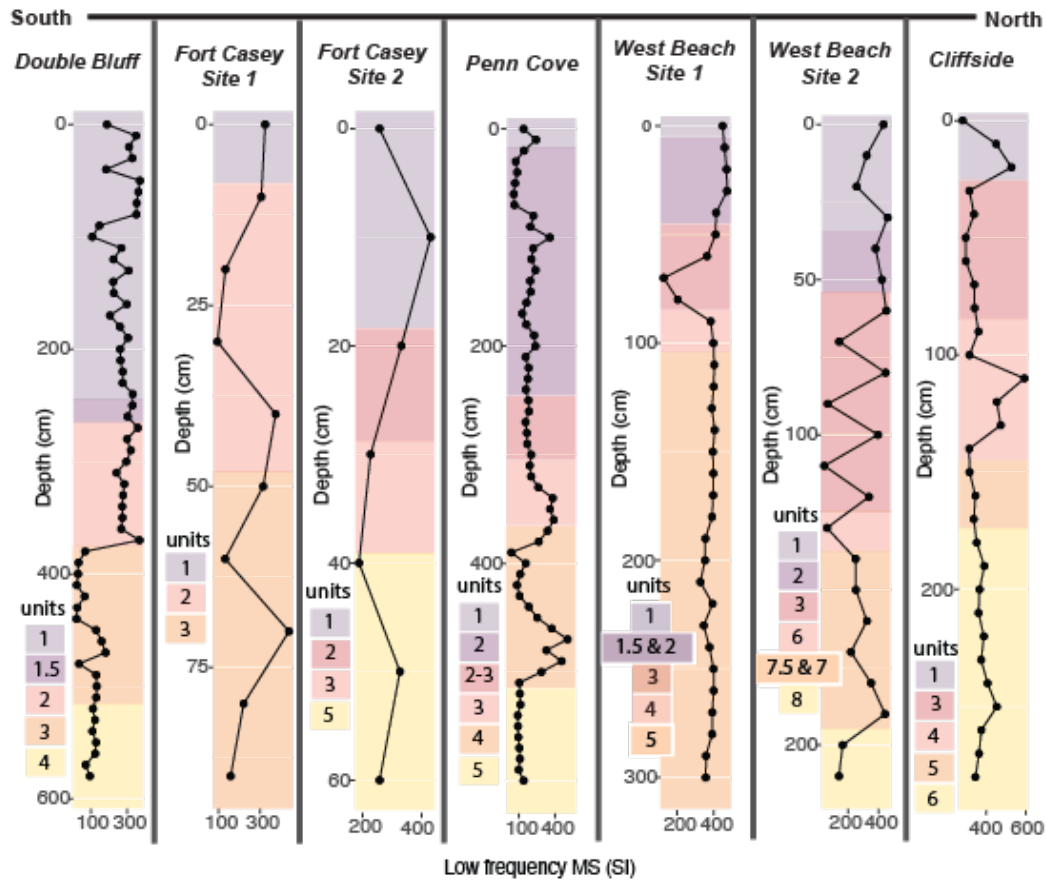


**Figure S2.** Magnetic susceptibility values for each site, listed south to north. Colored boxes indicate stratigraphic unit correlations. All site unit classifications are independent of one another. Variations in sampling resolution are a function of accessibility to outcrops from the beach front. Some units were more accessible for sampling than others.

75

**Table S1.** Site and sample collection information.

Site	Sediment samples	Radiocarbon samples	OSL samples
Double Bluff (a)	53	2	0
Fort Casey (b)	20	0	2
Penn Cove (c)	126	8	2
West Beach (d)	54	4	6
Cliffside (e)	29	0	0
<b>Total</b>	<b>282</b>	<b>14</b>	<b>12</b>

80 **Table S2.** Radiocarbon ages used to determine local marine reservoir effect (MRC).

Name	Type	Age $\pm$ error (RCY)	MRC	Age $\pm 2\sigma$ (cal year BP)	Time since live-collection (cal years BP)	NOSAMS Receipt #
Mo. r. 6298-1	live-collected bivalve	840 $\pm$ 15	236 $\pm$ 30	78 $\pm$ 112	91	176246
Mu. n. 3320-1	live-collected bivalve	860 $\pm$ 25	253 $\pm$ 51	90 $\pm$ 119	110	176247
Mu. n. 3320-2	live-collected bivalve	925 $\pm$ 20	318 $\pm$ 40	84 $\pm$ 115	110	176248
Ca.v. 13329-1	live-collected bivalve	875 $\pm$ 20	270 $\pm$ 40	83 $\pm$ 114	104	176249
Ca. v. 13329-2	live-collected bivalve	890 $\pm$ 15	285 $\pm$ 30	79 $\pm$ 112	104	176250
Ma. c. 3348-1	live-collected bivalve	895 $\pm$ 15	288 $\pm$ 30	80 $\pm$ 112	110	176251
Ma. c. 3348-2	live-collected bivalve	890 $\pm$ 20	283 $\pm$ 40	84 $\pm$ 115	110	176252
My. a. 3427-1	live-collected bivalve	905 $\pm$ 15	298 $\pm$ 30	80 $\pm$ 112	110	176253
My. a. 3427-2	live-collected bivalve	850 $\pm$ 20	243 $\pm$ 40	84 $\pm$ 115	110	176254
Ma. n. 3470-1	live-collected bivalve	825 $\pm$ 15	221 $\pm$ 30	78 $\pm$ 112	91	176255
Ma. n. 3470-2	live-collected bivalve	815 $\pm$ 15	211 $\pm$ 30	78 $\pm$ 112	91	176256

**Table S3.** OSL measurement sequence

- 85
1. Radiation dose  $D_i$
  2. Preheat at 180°C\* for 10s

3. IRSL at 125°C for 150s to remove feldspar signal  
 4. OSL at 125°C for 100s, measure OSL signal  $L_i$   
 5. Fixed test radiation dose  $D_t^{**}$   
 6. Cutheat at 160°C to remove unstable signals  
 90 7. IRSL at 125°C for 150s to remove feldspar signal  
 8. OSL at 125°C for 100s, measure OSL signal  $T_i$   
 9. Repeat steps 2-8 for cycle 0 and steps 1-8 for cycles 1-7  
 Cycle 0: Natural signal,  $D_0 = 0$  Gy with no administered dose  
 Cycle 1-5: Regenerative doses,  $D_1, D_2 < D_1 < D_3 < D_0 < D_4 < D_5$   
 95 Cycle 6: Dose recovery test,  $D_6 = D_4^{***}$   
 Cycle 7: Recycle test,  $D_7 = D_1^{***}$   
 Cycle 8: Recuperation test,  $D_8 = 0$   
 \* preheat temperature determined by plateau test  
 \*\*  $D_t = 15-20\% D_0$   
 100 \*\*\* administered to check the precision with which a known dose can be recovered

**Table S4.** Dose measurements calculated from OSL aliquots (Table 1). Fading rate is according to Auclair et al., 2003.

Sample	Sample #	grain size	n measured	n used	Dose (Gy)	fading rate (%/decade)
FCS1-OSL1	1	90-125	23	13	12.1 ± 2.8	7.1 ± 6.1
FCS2-OSL1	2	63-90	33	24	93.0 ± 7.3	3.6 ± 3.8
FCS2-OSL2	3	63-90	48	18	69.2 ± 4.6	2.7 ± 2.5
WBS1-OSL1	4	150-250	37	19	7.50 ± 0.68	2.6 ± 5.5
WBS1-OSL2	5	90-150	45	35	11.86 ± 0.68	0
WBS2-OSL1	6	90-212	49	34	64.6 ± 4.7	3.7 ± 2.5
WBS2-OSL2	7	90-150	37	26	71.0 ± 4.1	0
WBS3-OSL1	8	150-212	45	26	68.4 ± 5.0	0
WBS3-OSL2	9	150-212	56	29	55.9 ± 4.8	3.0 ± 1.7
PCS2-OSL1	10	125-150	50	28	75.5 ± 5.8	4.54 ± 0.28
PCS2-OSL2	11	125-150	38	32	93.2 ± 4.1	0

105 **Table S5.** Dose rate data calculated from OSL gamma samples.

Sample	Sample #	Th (ppm)	Th err	U* (ppm) Th234	U* err	U** (ppm) Pb, Bi	U** err	K (%)	K err	water***	DR cosm (mGy/a)	err	internal K factor****	err	DR gamma (mGy/a)	err	DR beta ext (mGy/a)	err	DR beta int (mGy/a)	err	DR total (mGy/a)	err
FCS1-OSL1	1	1.80	0.46	1.38	0.16	0.67	0.04	0.52	0.03	0.00	0.18	0.01	0.50	0.50	0.33	0.03	0.61	0.03	0.18	0.07	1.30	0.09
FCS2-OSL1	2	3.32	0.70	3.02	0.28	1.18	0.06	1.08	0.05	0.00	0.19	0.01	0.50	0.50	0.67	0.07	1.27	0.06	0.14	0.06	2.26	0.11
FCS2-OSL2	3	2.20	0.53	2.97	0.27	1.20	0.06	1.08	0.05	0.02	0.19	0.01	0.50	0.50	0.60	0.06	1.21	0.06	0.14	0.06	2.13	0.10
WBS1-OSL1	4	1.90	0.45	2.62	0.24	0.91	0.05	1.04	0.05	0.00	0.19	0.01	0.50	0.50	0.55	0.06	1.10	0.06	0.36	0.21	2.20	0.22
WBS1-OSL2	5	2.10	0.49	2.81	0.25	0.87	0.05	1.04	0.05	0.01	0.19	0.01	0.00		0.56	0.07	1.14	0.06	0.00		1.90	0.14
WBS2-OSL1	6	2.63	0.63	2.45	0.25	1.27	0.08	1.41	0.07	0.02	0.06	0.00	0.50	0.50	0.67	0.05	1.39	0.06	0.25	0.23	2.37	0.24
WBS2-OSL2	7	3.44	0.76	2.27	0.23	1.22	0.07	1.31	0.06	0.02	0.06	0.00	0.50	0.50	0.67	0.05	1.33	0.07	0.22	0.11	2.27	0.14
WBS3-OSL1	8	3.20	0.78	1.91	0.22	1.14	0.07	1.26	0.06	0.02	0.06	0.00	0.50	0.50	0.62	0.05	1.20	0.05	0.34	0.04	2.23	0.08
WBS3-OSL2	9	3.71	0.82	2.62	0.26	1.30	0.07	1.40	0.07	0.02	0.06	0.00	0.50	0.50	0.73	0.06	1.42	0.06	0.25	0.07	2.47	0.11
PCS2-OSL1	10	2.22	0.48	1.93	0.18	0.88	0.05	0.94	0.05	0.01	0.13	0.01	0.90	0.10	0.49	0.04	0.97	0.04	0.45	0.07	2.05	0.10
PCS2-OSL2	11	2.00	0.48	1.88	0.19	0.90	0.05	1.00	0.05	0.00	0.13	0.01	0.90	0.10	0.50	0.04	1.02	0.05	0.45	0.07	2.10	0.10

\*Uranium in ppm, based on Th<sup>234</sup>

\*\*Uranium in ppm, based on Pb<sup>214</sup> and Bi<sup>214</sup>

\*\*\*water content as measured from the wet and dry samples; it seems that the samples were nearly dry; water content is around 1-2%; uncertainty was assumed to be 5% of the measured value.

110 \*\*\*\*fraction of feldspar in the quarts; for most samples this value was assumed to be 50% with an uncertainty of 50% (i.e., the value could be anywhere between 0 and 100%).

## References

- 115 Auclair, M., Lamothe, M., and Huot, S.: Measurement of anomalous fading for feldspar IRSL using SAR, *Rad. Measurements*, 37(4), 487–492, [https://doi.org/10.1016/S1350-4487\(03\)00018-0](https://doi.org/10.1016/S1350-4487(03)00018-0), 2003.
- Barbouti, A. I., and Rastin, B. C.: A study of the absolute intensity of muons at sea level and under various thicknesses of absorber, *J Phys G: Nuclear Phys*, 9(12), 1577, <https://doi.org/10.1088/0305-4616/9/12/018>, 1983.
- Bøtter-Jensen, L., and Murray, A. S.: Developments in Optically Stimulated Luminescence Techniques for Dating and Retrospective Dosimetry, *Rad Protection Dosimetry*, 84(1), 307–315, <https://doi.org/10.1093/oxfordjournals.rpd.a032745>, 1999.
- 120 Galbraith, R. F., Roberts, R. G., Laslett, G. M., Yoshida, H., and Olley, J. M.: Optical dating of single and multiple grains of quartz from Jinmium rock shelter, Northern Australia: Part 1, Experimental design and statistical models, *Archaeometry*, 41(2), 339–364, <https://doi.org/10.1111/j.1475-4754.1999.tb00987.x>, 1999.
- Guérin, G., Mercier, N., and Adamiec, G.: Dose-rate conversion factors: update, *Ancient TL* 29(1), 5-8, 2011.



- 125 Murray, A. S., and Wintle, A. G.: Luminescence dating of quartz using an improved single-aliquot regenerative-dose protocol, *Rad. Measurements*, 32(1), 57–73, [https://doi.org/10.1016/S1350-4487\(99\)00253-X](https://doi.org/10.1016/S1350-4487(99)00253-X), 2000.
- Prescott, J. R., and Hutton, J. T.: Cosmic ray contributions to dose rates for luminescence and ESR dating: Large depths and long-term time variations, *Rad. Measurements*, 23(2), 497–500, [https://doi.org/10.1016/1350-4487\(94\)90086-8](https://doi.org/10.1016/1350-4487(94)90086-8), 1994.
- Prescott, J. R., and Stephan, L. G.: The contribution of cosmic radiation to the environmental dose for thermoluminescence dating, *PACT*, 6, 17–25. <https://cir.nii.ac.jp/crid/1573668924373277824>, 1982.
- 130 Wallinga, J., S. Murray, A., and Bøtter-Jensen, L.: Measurement of the Dose in Quartz in the Presence of Feldspar Contamination, *Rad. Protec. Dosimetry*, 101(1), 367–370, <https://doi.org/10.1093/oxfordjournals.rpd.a006003>, 2002.
- Wintle, A. G., and Murray, A. S.: A review of quartz optically stimulated luminescence characteristics and their relevance in single-aliquot regeneration dating protocols, *Rad. Measurements*, 41(4), 369–391, <https://doi.org/10.1016/j.radmeas.2005.11.001>, 2006.

135